

# Electrodynamics Optimization Reflected Intensity of Linearly Polarized Electromagnetic Plane Wave from a Parabolic Cylinder Boundary Interface between Two Different Optical Mediums

Hossein Arbab<sup>1</sup>, Mehdi Rezagholizadeh<sup>2</sup>

<sup>1</sup>*Department of physics, Faculty of Science, University of Kashan, Kashan, Isfahan state, I. R. of Iran*

<sup>2</sup>*Center of intelligent Machines, Department of electrical and computer engineering, McGill University, Quebec, Canada*

**Abstract-** The aim of this study is investigate the dependence of reflected intensity of linearly polarized electromagnetic plane wave from a parabolic cylinder boundary interface. The opening area of device is kept constant but its focal length would be changed. For this purpose, a discrete mathematical modeling is applied. We apply this model to a non - integrated parabolic mirror as well as a smooth and continuous one. In this model a cylindrical parabolic reflector is divided into definite number of thin long strips (number of strips depends on the focal length of device and width of the strips). Such a model is chosen, because it would be matched with an innovative fabrication method of a special type of parabolic mirror which is fabricated on the basis of this method. This method of fabrication has been published in details for circular parabolic mirrors in the journal of optics (optical society of India). At the present paper we investigate optimum reflected power by a parabolic trough interface between two different optical mediums. Results of calculations show that if the opening area of interface is kept constant but its focal length is changing, then reflected power would be depended on the focal length of the parabolic mirror, optical properties of the reflecting surface, state of polarization of incoming wave, configuration of interface with plane of incidence and wavelength of the incoming wave. Subject of this article is important, because it would be applied to many high-tech instruments in the fields of science and technology. For example radio telescope and reflective telescope in astronomical science concave and convex lenses and any kind of curved mirrors in the field of optics, solar furnace, satellite, radar and parabolic telecommunication antennas in the field of engineering.

**Keywords:** Electromagnetic plane wave, Radio Telescope, Polarization, Fresnel Coefficients, Parabolic Mirror, Plane of Incidence, Solar Energy

## I. INTRODUCTION

Importance and key role of the kinds of parabolic reflectors and other optical elements such as lenses aren't hidden in various scientific and applied fields of optics. There are many examples on the various fields of applied physics that they show the importance of the subject: Radio telescope and parabolic mirrors of reflecting telescopes on the field of astronomical researches, parabolic antennas of satellite receivers on the field of communication, radar antennas in the field of tracking and tracing, concave and convex lenses in the field of optical instruments and parabolic mirrors of the solar dishes in the field of renewable energies are all examples which reveal the high importance of the subject of current article. In this article we will show that in order to get optimum utilization of curved reflectors (and lenses) it is necessary to note the detailed features of electrodynamics and geometrical structure of these instruments. In fact, we are studying the behavior of a parabolic cylindrical reflector with particular attention to the reflected back power of incoming beam at the focal line. So it is of vital importance to design instruments with optimum output and get access new methods to exploit solar radiation. In the field of renewable energies, undoubtedly huge amount of energy is reaching to our planet due to sun radiation every day. Average solar energy flux on the earth surface is measured about 1367 watts per square meter [1]. On the other hand parabolic mirror is also an important component of many solar energy systems. Moreover parabolic cylindrical reflector focuses the sunlight onto a linear tube located at its focal line that contains a working fluid. The working fluid absorbs the solar energy and carries it to some thermal plant, such as a sterling heat engine [2]. The mirror shape must be precise enough to ensure that the reflected sunlight is focused on the absorber tube .There are important practical reasons to keep the size of absorber tube small. For example coast, thermal radiation and convection losses [3] are some of important reasons that are caused the size of absorber tube to be small. Also a solar dish concentrator may be used in the process of hydrogen production at high temperature [4, 5] or even is

applied as an instrument for surgery in the branch of medical sciences [6]. In order to optimize the device, theoretical analysis of thermodynamic limit of concentration [7, 8] and cavity optimization [9] are the important issues where have been investigated by scientists and engineers previously. Furthermore, several methods of optimizing performance of solar dishes has been proposed from different point of views such as certain optical properties of the reflecting material [10], dependence of optical efficiency to the incident angle [11], and increasing the concentration ratio and obtaining the uniform illumination distribution for PV cells [12]. Optimizing the parabolic mirrors on the basis of its geometrical structure and electro-dynamics point of view is the newest and update subject in this field which was considered in details (for circular parabolic mirror) and published firstly by author in journal of optics [13]. Now in the course of this activity we investigate reflected energy distribution due to variation of focal length of parabolic cylindrical interface of two different optical mediums, polarization states of incident wave and order of the optical mediums. But it must be noted that solar parabolic reflectors are constructed in different shapes and structures. A fantastic typical method of construction of parabolic mirror which is based on laser spot image processing has been published previously in journal of optics [14]. In this article we choose mathematical optimization modeling such that the simulation to be consistent completely with procedure of fabrication method. Of course, it must be noted that the discrete model which is presented in this paper is applicable to a smooth and continuous parabolic cylindrical interface. Also the narrow strips elements could be chosen from an arbitrary conductor or dielectric material. Finally the fabricated reflector has the advantages of simplicity and accuracy and is capable of tracking the sun using an innovative intelligent controller based on the image processing of bar shadow [15]. Before entering the main discussion of our work, it is necessary to introduce an explicit explanation of the parabolic cylindrical structure. The rectangular elements (strips) of our device are installed on the base of a parabolic cylinder. The distances of strips are different from symmetrical plane of device. The number of these elemental surfaces which are covering the parabolic substrate is a function of width of strips and the focal length of parabola. In our work, the opening diameter of the parabolic cylinder is kept constant, but its focal length would be changed. The variation of focal length not only affects the number of strips but also the total reflected power of **S** and **P** polarization states at the focal line are changed. This work is organized in four sections. The introduction is presented as Section 1. Section 2 is devoted to the mathematical modeling and analytical calculations. In Section 3 simulation is done and diagrams of the reflected energy distribution is presented. Finally, in Section 4 a summary and conclusion are proposed.

## II. MATHEMATICAL MODELING AND ANALYTICAL CALCULATIONS

In general point of view, the structure of a reflecting surface may be taken smooth and continues or non-integrated. The non-integrated one not only describes the practical type has been made by author accurately, but also it can be a good approximation of continues one (when the number of strip elements goes to infinity). Physically, the Fresnel reflecting coefficients depend on the angle of incidence, therefore these coefficients is changed from a certain strip to another one. In addition the amount of falling radiation on a definite strip of the device is a function of focal length. Fig.1

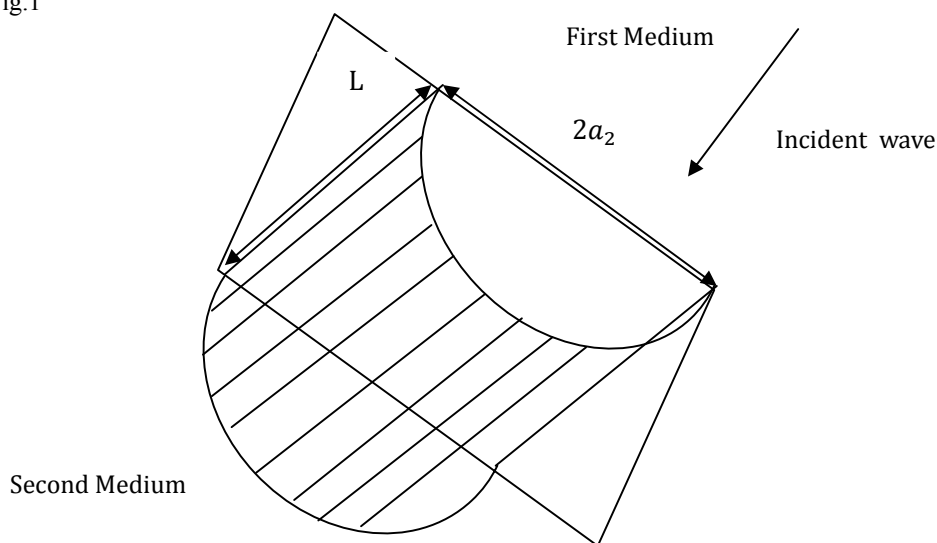
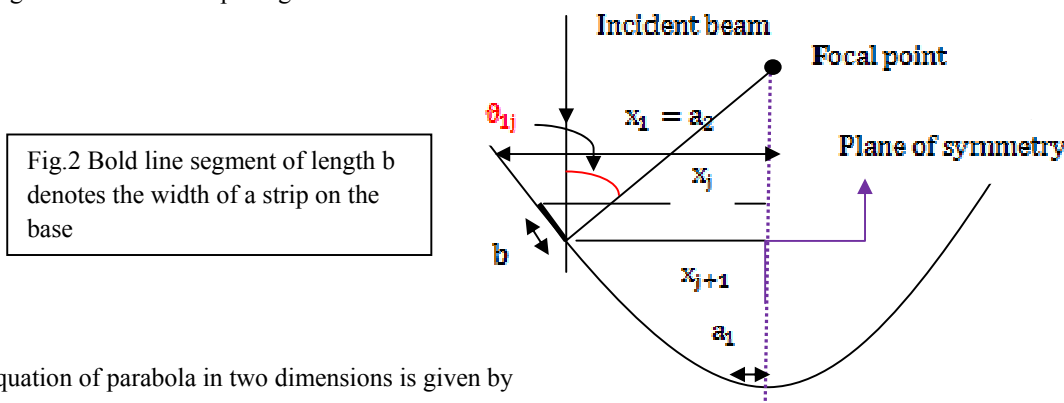


Fig. 1. parabolic trough interface separates two different optical Mediums

It is important to note that in order to test the results of our mathematical modeling, at the first step we assume the parabolic cylinder interface between two semi- infinite optical mediums such as vacuum and glass. Simple mathematical calculations show that the number of strips on the boundary interface of two mediums is integer part of  $N(f)$  which is given by

$$N(f) = \frac{a_2}{b} \sqrt{1 + \left(\frac{a_2}{2f}\right)^2} + \frac{2f}{b} \sinh^{-1}\left(\frac{a_2}{2f}\right) - \frac{a_1}{b} \sqrt{1 + \left(\frac{a_1}{2f}\right)^2} - \frac{2f}{b} \sinh^{-1}\left(\frac{a_1}{2f}\right) \quad (1)$$

Where  $a_2$ ,  $b$ ,  $f$ , and  $a_1$  are denoting the half width of the opening diameter, the width of strips, focal length of parabola and half width of the shaded region at the vertex respectively. Let  $x_j$  be the distance of the  $j$ th strip from the symmetrical plane of the parabola. The relation (1) simply shows that the number of strips is function of focal length and width of strips. Fig2



Equation of parabola in two dimensions is given by

$$y(x) = \frac{x^2}{4f} \quad (2)$$

It can be shown simply that the angle of inclination of the  $j$ th strip is given by

$$\tan \theta_{1j} = \frac{x_j}{2f} \quad (3)$$

There are two different methods of enumerating the number of strips. Counting the number of strips may be done from the opening to the vertex and vice versa. By counting the number of strips from opening to the vertex, the dependence  $x_{j+1}$  on  $x_j$  is determined by a recurrent formula as follows

$$x_{j+1} = x_j - \frac{b}{\sqrt{1 + \left(\frac{x_j}{2f}\right)^2}} \quad j = 1, 2, \dots, \left[\frac{N(f)}{2}\right], \quad x_1 = a_2 \quad (4)$$

Now we calculate  $F_s$  and  $F_p$ , the reflected power of **S** and **P** polarization states respectively in the following situations

- 1) E oscillates in the **XOZ**, the symmetrical plane of parabolic cylinder boundary interface. Fig.3a **E = E<sub>s</sub> and  $\varphi = 0$**
- 2) E oscillates in the **YOZ**, **E = E<sub>p</sub> and  $\varphi = \frac{\pi}{2}$** , Fig.3b

3) E oscillates in an arbitrary plane which has an angle  $\varphi$  from the plane **XOZ**, Fig.4  
 $0 \leq \varphi \leq 2\pi$

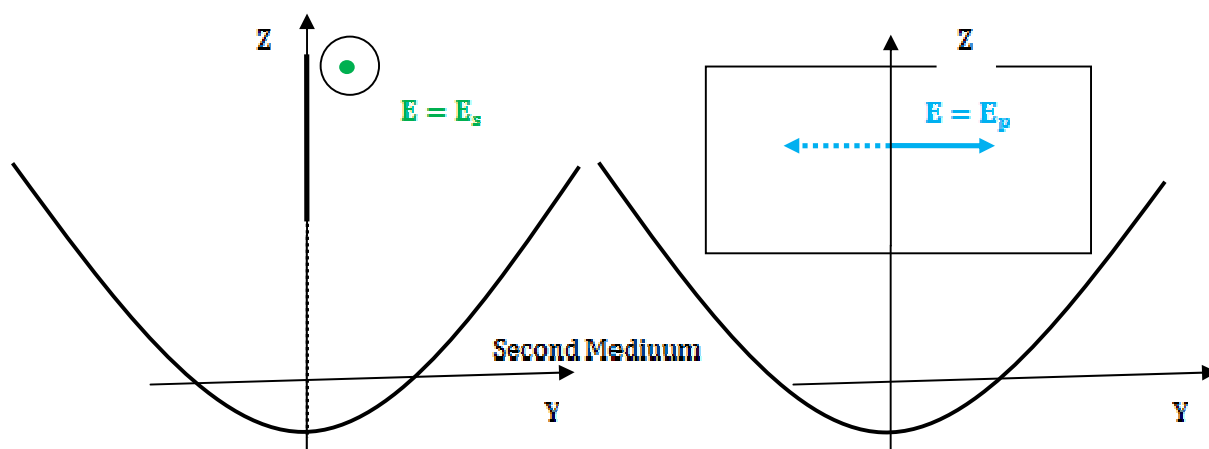


**Fig. 3a** Cross section of boundary interface of parabolic trough is shown. E is perpendicular to the plane of incidence and oscillates in the **XOZ**, symmetry plane of boundary surface.

**Fig. 3b** E is parallel to the plane of incidence and oscillates in the **YOZ**

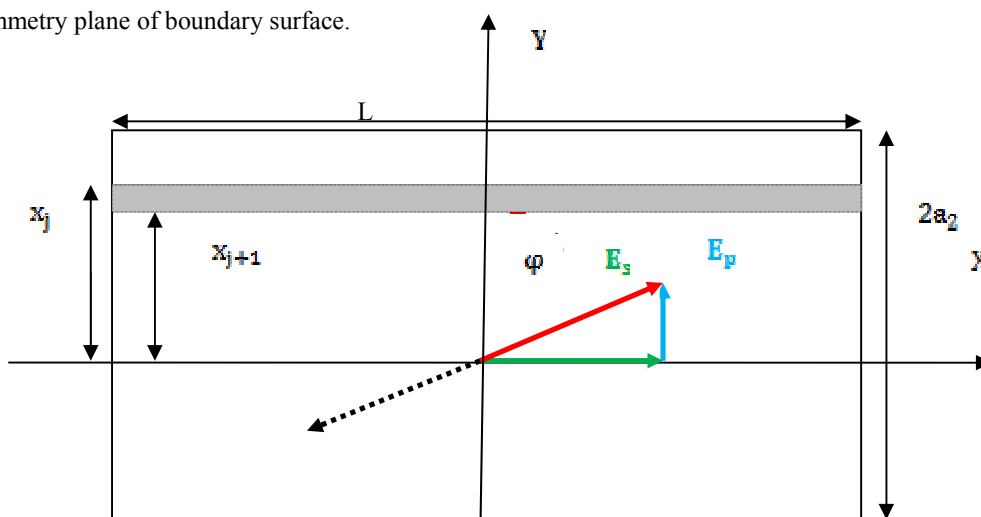


**Fig.4** Opening of the parabolic trough interface is parallel with **XOY** plane. One of the strips is shown in gray color.

1) Electromagnetic field vector E oscillates in the plane of symmetry of parabolic cylinder  $\mathbf{E} = \mathbf{E}_s$   
 As the figure 3a shows, in this situation vector E oscillates in a plane which is normal to the plane of incidence.

Therefore E has only **S** component and we consider three following cases:

(1-A) Parabolic cylinder boundary surface separates vacuum from glass medium (Electromagnetic source of wave is placed in vacuum)

(1-B) Parabolic cylinder boundary surface separates glass from vacuum (Electromagnetic source of wave is placed in glass)

(1-C) Parabolic cylinder boundary surface separates vacuum from a conductor medium (Electromagnetic source of wave is placed in vacuum)

(1-A) The electromagnetic source of wave is placed in vacuum

We assume that an incident plane polarized electromagnetic wave moves (along the symmetrical plane) from the first medium (vacuum) into the second one (glass). Merely when  $f$  goes to infinity ( $f \rightarrow \infty$ ) we have a special

case where the boundary interface would be a flat surface. Therefore a fraction of incident power would be passed into the second medium and its remainder reflected back to the vacuum. (In this situation the numerical value of reflected and transmitted intensity would be calculated simply) To calculate reflected power of the wave back to the first medium (vacuum) the Fresnel reflection coefficients should be determined [16].

$$r_{12s} = \frac{n_1 \cos \theta_1 - n_2 \cos \theta_2}{n_1 \cos \theta_1 + n_2 \cos \theta_2} \quad \text{for S polarization} \quad (5)$$

$$r_{12p} = \frac{n_2 \cos \theta_1 - n_1 \cos \theta_2}{n_2 \cos \theta_1 + n_1 \cos \theta_2} \quad \text{for P polarization} \quad (6)$$

( $n_1, n_2$  are reflection index of the first and second medium respectively)  
 For normal incident we have:

$$\theta_1 = \theta_2 = 0 \quad (7)$$

In this article index 1 stands to the first medium (medium which the source of wave is placed in) and index 2 stands to the second medium. Therefore

$$r_{12s} = -r_{12p} = \frac{n_1 - n_2}{n_1 + n_2} \quad (8)$$

$$R_s = R_p = \left( \frac{n_1 - n_2}{n_1 + n_2} \right)^2 \quad (9)$$

$R_s$  and  $R_p$  are the reflection coefficients for S and P polarization respectively. Suppose that  $L$  is the length of parabolic cylinder, then reflected power back to the vacuum is given by

$$F_p(\infty) = F_s(\infty) = 2L(a_2 - a_1)IR_s = 2L(a_2 - a_1)IR_p \quad (10)$$

Where  $F_s(\infty)$  and  $F_p(\infty)$  are the reflected power of S and P Polarization states respectively. Quantity  $I$  denotes irradiance of the incident wave. As we expect in normal incidence these two polarization states would be indistinguishable. We assume the following numerical values for given parameters:

$$n_1 = 1, n_2 = 1.5, I = 1000 \text{ W/m}^2, a_1 = .01\text{m}, a_2 = 1\text{m}, b = .001\text{m}, L = 10\text{m}$$

From (9) and (10) the reflected power back to the vacuum is given by

$$F_p(\infty) = F_s(\infty) = 2 \times 10 \times (1 - 0.01) \times 1000 \times \left( \frac{1 - 1.5}{1 + 1.5} \right)^2 = 792 \text{ W} \quad (11)$$

(Note that the corresponding numerical values are chosen for simplicity)

In order to investigate an accurate analysis for a special type of cylindrical parabolic mirror has been made by author, it is necessary to use a suitable mathematical model which is applicable to this structure. To control this issue

we note the numerical value is given by (11). Now assume that the plane polarized electromagnetic wave propagates along the plane of symmetry toward the parabolic cylinder boundary interface. We divide boundary surface of the parabolic cylinder to small strips as shown in Fig.1

It must be note that angle  $\theta_{1j}$  of the incident wave is changing from a certain strip to another one. Using equations (5), (6) and Snell law and we obtain

$$r_{12sj} = \frac{n_1 \cos \theta_{1j} - n_2 \left[ 1 - \left( \frac{n_1}{n_2} \right)^2 \sin^2 \theta_{1j} \right]^{\frac{1}{2}}}{n_1 \cos \theta_{1j} + n_2 \left[ 1 - \left( \frac{n_1}{n_2} \right)^2 \sin^2 \theta_{1j} \right]^{\frac{1}{2}}} \quad (12)$$

$$r_{12pj} = \frac{n_2 \cos \theta_{1j} - n_1 \left[ 1 - \left( \frac{n_1}{n_2} \right)^2 \sin^2 \theta_{1j} \right]^{\frac{1}{2}}}{n_2 \cos \theta_{1j} + n_1 \left[ 1 - \left( \frac{n_1}{n_2} \right)^2 \sin^2 \theta_{1j} \right]^{\frac{1}{2}}} \quad (13)$$

Thus for reflection coefficients of S and P polarization states we have

$$R_{sj} = r_{12sj}^2 \quad (14)$$

$$R_{pj} = r_{12pj}^2 \quad (15)$$

Irradiance of polarization states S and P are given by

$$I_{sj} = I \cos^2 \phi \quad (16)$$

$$I_{pj} = I \sin^2 \phi \quad (17)$$

Then the total energy flux of S and P polarization reflected back to focal line is given by

$$F_s(f) = 2 \sum_{j=1}^{\left[ \frac{N(f)}{2} \right]} I_{sj} R_{sj} bL \cos \theta_{1j} \quad (18)$$

$$F_p(f) = 2 \sum_{j=1}^{\left[ \frac{N(f)}{2} \right]} I_{pj} R_{pj} bL \cos \theta_{1j} \quad (19)$$

Results of calculations are shown by Figs .5a and 5b

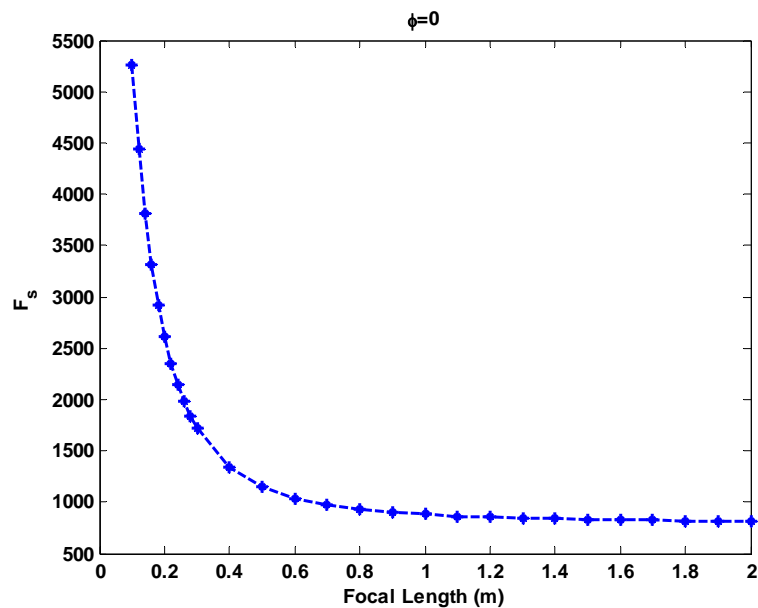


Figure 5a

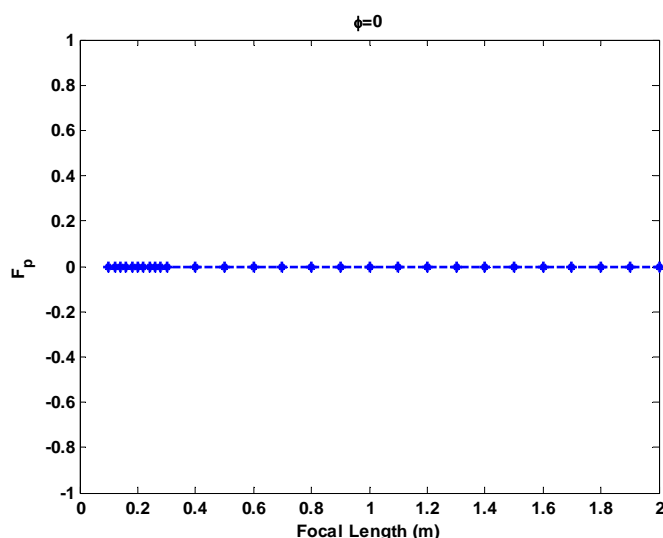


Figure 5b

Figure 5a shows if  $f \rightarrow \infty$  there is a good agreement between numerical value was given by (11)  
 (1-B)The electromagnetic source of wave is placed in the glass (dense medium)

At this step we assume that the dense medium (glass) is first medium and vacuum is the second one. The incident electromagnetic wave propagates in parallel with the plane of symmetry toward the common parabolic cylinder boundary interface. Because of total internal reflection in this situation calculations would be a little different from that one was done in (1-A). In this case we must care with total internal reflection. The critical angle is given by

$$\theta_c = \sin^{-1} \frac{n_2}{n_1} \tag{20}$$

We must consider total internal reflection for those of strips which satisfying the following relation

$$\theta_{1j} > \theta_c \tag{21}$$

In this case results of computer calculations are shown by Figs.6a and 6b

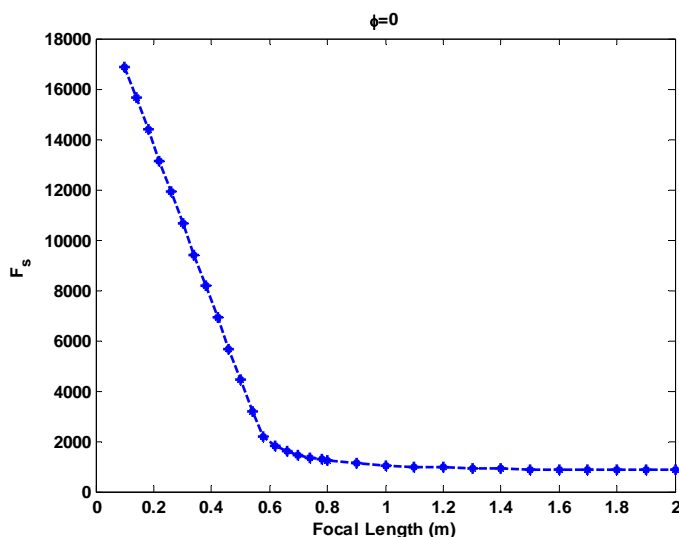


Figure 6a

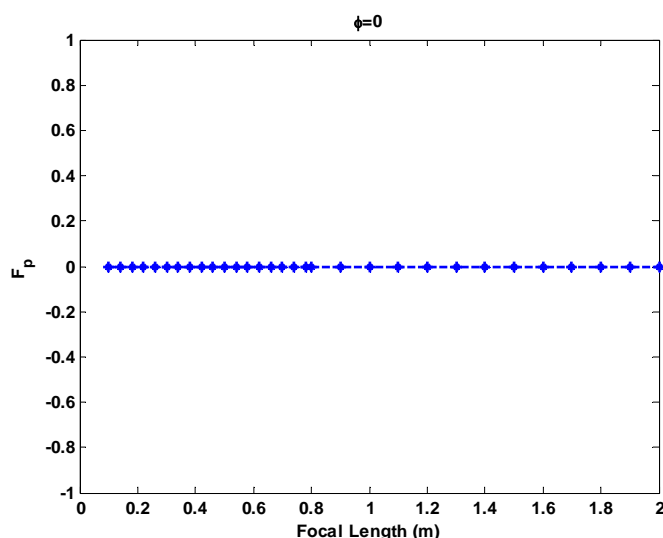


Figure 6b

(1-C)The electromagnetic source of wave is placed in vacuum (parabolic boundary separates vacuum and conductor)

In this case we encounter a more practical situation that our cylindrical parabolic mirror includes a number of conducting strips without any protecting covers. Numerical results was derived in subsections (1-A) and (1-B) established that the mathematical modeling gives acceptable values in the limiting conditions. So, now we can use this mathematical model to analyze the structure of discrete (and continuous) cylindrical parabolic mirror. As before, we assume that the incident wave moves parallel with the plane of symmetry from vacuum (first medium) to the second one (conductor). The Fresnel reflection amplitude coefficients for **S** and **P** polarizations are given by the following relations respectively

$$\tilde{r}_{12sj} = \frac{n_1 \cos \theta_{1j} - \tilde{n}_2 \cos \tilde{\theta}_{2j}}{n_1 \cos \theta_{1j} + \tilde{n}_2 \cos \tilde{\theta}_{2j}} \quad (22)$$

$$\tilde{r}_{12pj} = \frac{\tilde{n}_2 \cos \theta_{1j} - n_1 \cos \tilde{\theta}_{2j}}{\tilde{n}_2 \cos \theta_{1j} + n_1 \cos \tilde{\theta}_{2j}} \quad (23)$$

Where  $\tilde{\theta}_{2j}$  denotes complex angle in the second medium (conductor) and  $\tilde{n}_2$  is complex refraction index and depends on  $n_2$  and  $k_2$  are known as conductor optical constants:

$$\tilde{n}_2 = n_2 + i k_2 \quad (24)$$

Complex propagation wave vector in *j*th conducting strip is denoted by  $\tilde{k}_{2j}$ . The complex angle  $\tilde{\theta}_{2j}$  is defined by following relations:

$$\tilde{k}_{2j} \cdot \hat{n} = \tilde{k}_{2j} \cos \tilde{\theta}_{2j} \quad (25)$$

$$\tilde{n}_2 \cos \tilde{\theta}_{2j} = \beta_j + i \gamma_j \quad (26)$$

Where

$$\beta_j = \left\{ \frac{1}{2} \left[ n_2^2 - k_2^2 - n_1^2 \sin^2 \theta_{1j} + \sqrt{(n_2^2 - k_2^2 - n_1^2 \sin^2 \theta_{1j})^2 + 4n_2^2 k_2^2} \right] \right\}^{\frac{1}{2}} \quad (27)$$



$$\gamma_j = \left\{ \frac{1}{2} \left[ - (n_2^2 - k_2^2 - n_1^2 \sin^2 \theta_{1j}) + \sqrt{(n_2^2 - k_2^2 - n_1^2 \sin^2 \theta_{1j})^2 + 4n_2^2 k_2^2} \right] \right\}^{\frac{1}{2}} \quad (28)$$

$$j = 1, 2, 3, \dots, [N(f)]$$

Then from (23-25), and (27-29) we obtain the following formulas for Fresnel reflection amplitude coefficients.

$$\tilde{r}_{12pj} = \frac{[(n_2^2 - k_2^2) \cos \theta_{1j} - n_1 \beta_j] + i[2n_2 k_2 \cos \theta_{1j} - \gamma_j n_1]}{[(n_2^2 - k_2^2) \cos \theta_{1j} + n_1 \beta_j] + i[2n_2 k_2 \cos \theta_{1j} + \gamma_j n_1]} \quad (29)$$

$$\tilde{r}_{12sj} = \frac{[n_1 \cos \theta_{1j} - \beta_j] - i\gamma_j}{[n_1 \cos \theta_{1j} + \beta_j] + i\gamma_j} \quad (30)$$

Fresnel coefficients for P and S polarizations on  $j^{\text{th}}$  strip are given by

$$R_{pj} = \tilde{r}_{12pj} \tilde{r}_{12pj}^* \quad (31)$$

$$R_{sj} = \tilde{r}_{12sj} \tilde{r}_{12sj}^* \quad (32)$$

(Star sign is stand for complex conjugate) For **S** and **P** polarizations we can obtain the total power at focal line by equations (18) and (19) respectively. Consider a parabolic cylindrical mirror has been made from the strips of a nonmagnetic reflecting conductor such as silver. The optical constants for Ag (in visible spectrum) is  $n=0.05$ ,  $k=3$  [17]. Results of computer programming are shown by the figures 7a and 7b.

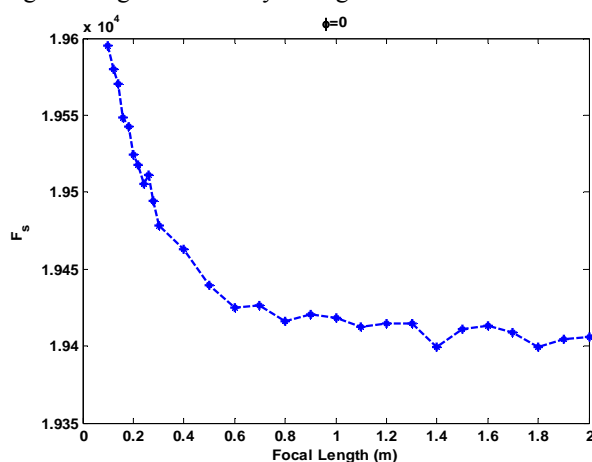


Figure 7a

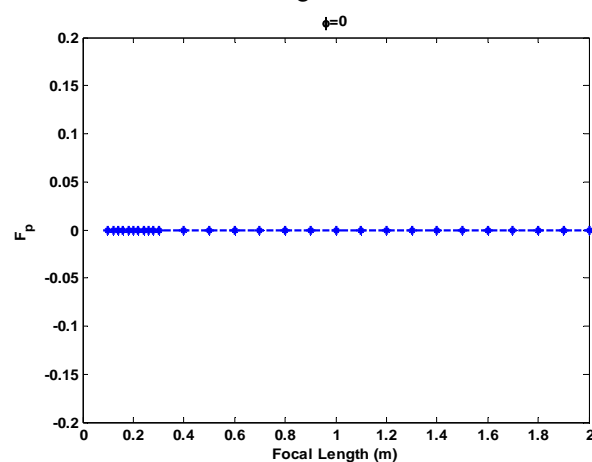


Figure 7b

When the focal length of parabolic cylinder is changing, its surface would not be covered completely by an integer number of elemental strips. Only for certain amounts of  $f$  the number of strips (which is given by relation (1)) would be an integer number. In general, for a given  $f$  a fraction of the last strip would be omitted. Therefore the smoothness of diagrams would be disturbed due to the operation of integer part (as the upper limit of summations). Because of small amounts of reflection amplitudes in subsections (1-A) and (1-B) this issue doesn't affect the smoothness of diagrams seriously. On the other hand when we use conductor elemental strips on the parabolic cylinder reflection amplitudes almost are close to one. Therefore cutting a section of an elemental strip due to the operation of integer part causes a jump on the diagram. Thus smoothness of the diagrams has been shown by figures 5a and 6a must be more than the smoothness of diagrams has been shown by figures 7a and 10a as is expected.

$$\mathbf{E} = \mathbf{E}_p$$

Electromagnetic field vector  $\mathbf{E}$  oscillate in the plane of incidence

As before we study this situation for the following cases

The electromagnetic source of wave is located in the vacuum

Computer calculations are based on the equations (1), (3), (4), (13), (15), and the following numerical values:

$$n_1 = 1, n_2 = 1.5, I = 1000 \text{ W/m}^2, a_1 = .01\text{m}, a_2 = 1\text{m}, b = 0.001\text{m}, L = 10\text{m}$$

Results of simulations are given by figures 8a and 8b:

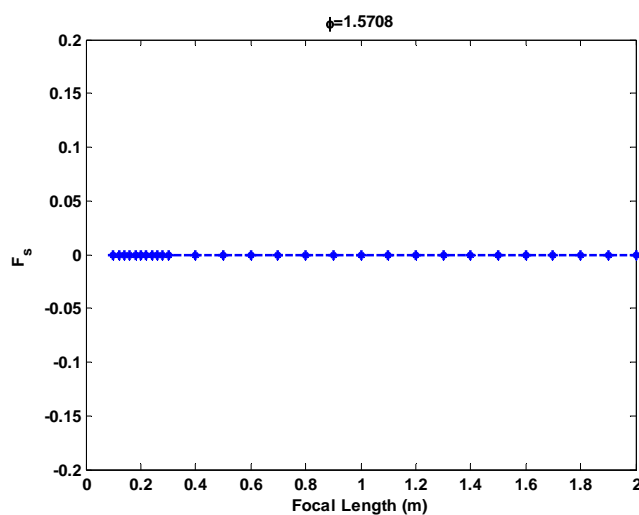


Figure 8a

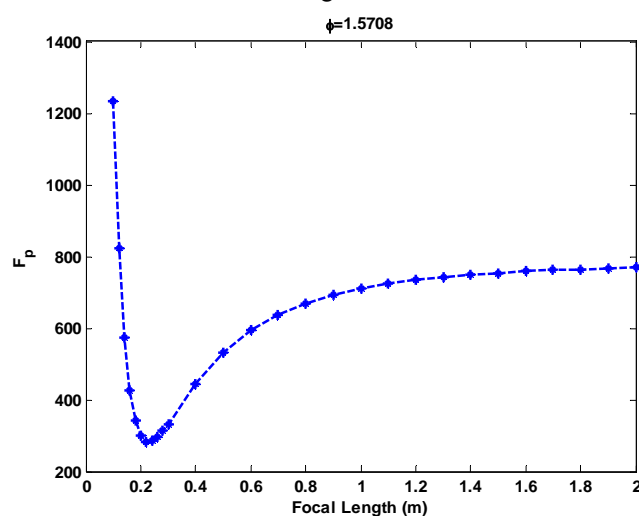


Figure 8b

The electromagnetic source of wave is located in dense medium

The critical angle is given by (20) and when  $\theta_{1i} > \theta_c$  total internal reflection would be taking placed. Calculations are based on the equations (1), (3), (4), (13), (15), (19), (20), and (21). Figures 9a and 9b show the results of computer programming.

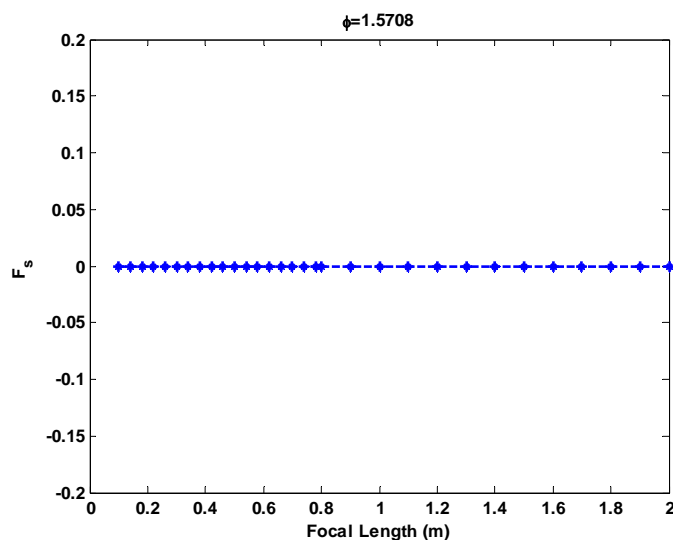


Figure 9a

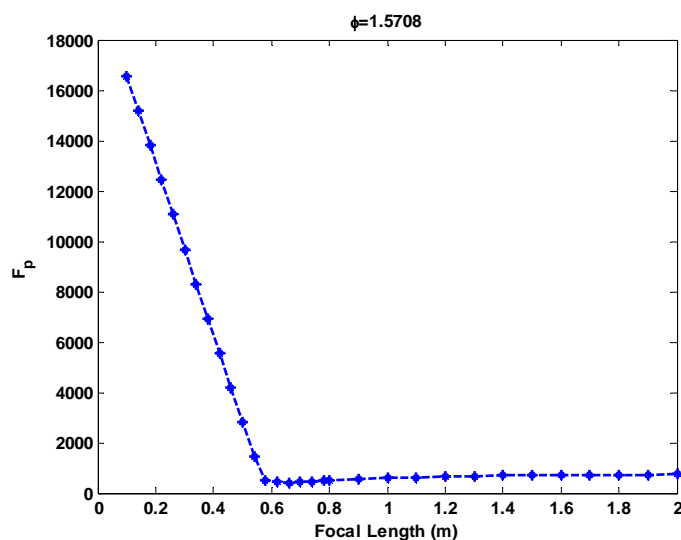


Figure 9b

The electromagnetic source of wave is placed in the vacuum (parabolic surface is located between vacuum and conductor)

Calculations are based on the equations (1), (3), (4), (13), (15), (29), (31)

Results of computer programming are given by figures 10a, 10b

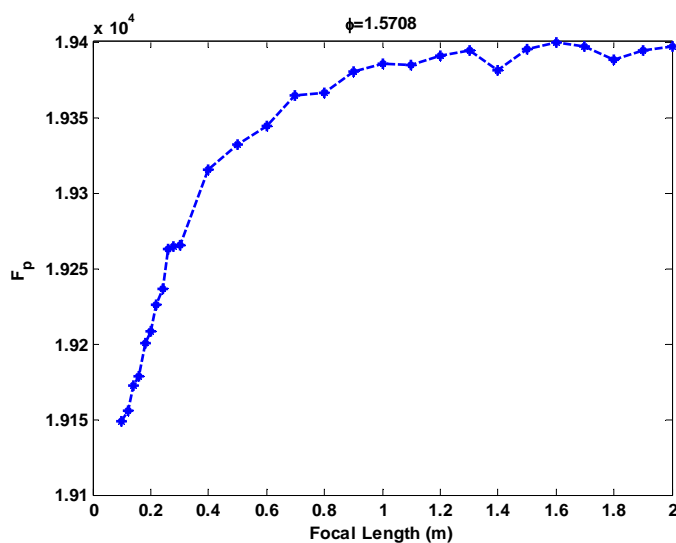


Figure 10a

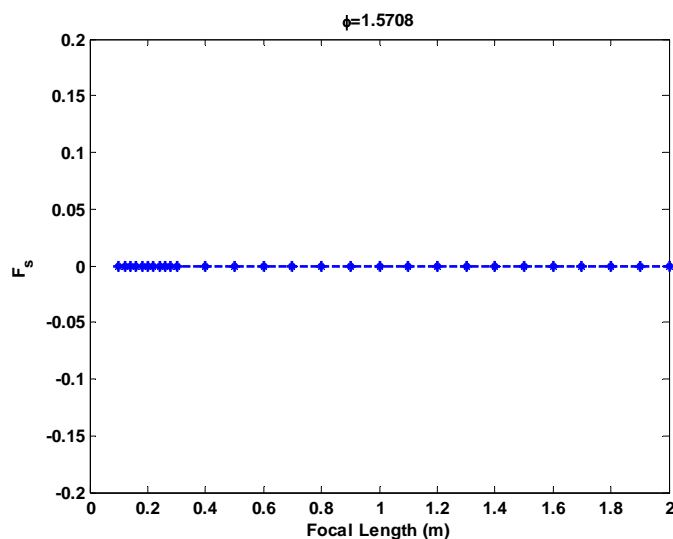


Figure 10b

### III. ELECTROMAGNETIC FIELD VECTOR $\mathbf{E}$ OSCILLATES IN AN ARBITRARY PLANE WHICH HAS AN ANGLE $\phi$ WITH THE PLANE $\mathbf{XOZ}$ AND IT IS PERPENDICULAR TO THE OPENING OF PARABOLIC CYLINDER

The electromagnetic wave source is in vacuum

The electromagnetic wave source is in glass

The electromagnetic wave source is in vacuum (parabolic boundary surface between vacuum and conductor)

Fig.4 shows a more general case that the incident wave has two polarization states S and P at the same time. It is

clear that both  $\mathbf{E}_s$  and  $\mathbf{E}_p$  are depend on angle  $\phi$ . We obtain the following relations for reflected intensities at the focal line:

$$F_s(f, \phi) = 2 \sum_{j=1}^{\lfloor \frac{N(f)}{2} \rfloor} I_{sj} R_{sj} bL \cos \vartheta_{1j} \quad (33)$$

$$F_p(f, \varphi) = 2 \sum_{j=1}^{\lfloor \frac{N(\varphi)}{2} \rfloor} I_{pj} R_{pj} bL \cos \vartheta_{1j} \quad (34)$$

From equations (33) and (34) we see clearly that powers  $F_E$  and  $F_P$  are depending not only on the angle  $\varphi$  but also on the focal line.

3.1 The electromagnetic wave source is in the vacuum

Calculations are based on the relations (33), (12), (14), (4), (3), (1). Results of simulations are shown in figures 11a and 11b

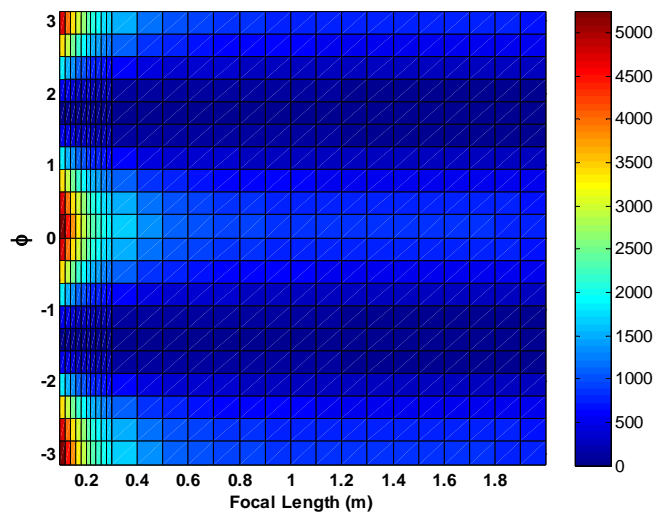
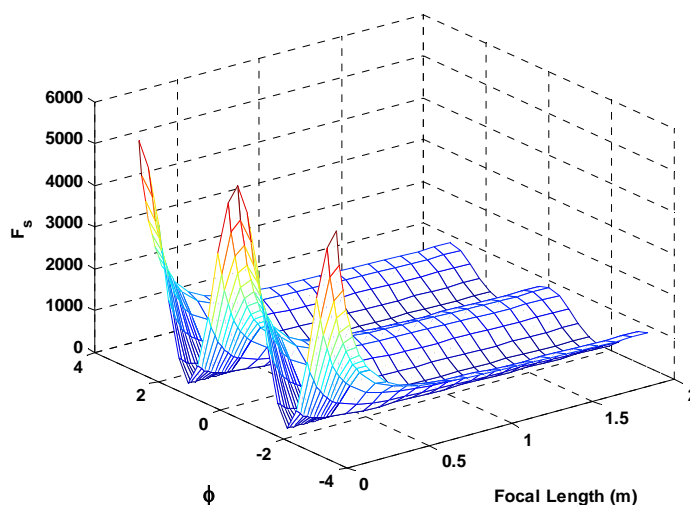


Figure 11a

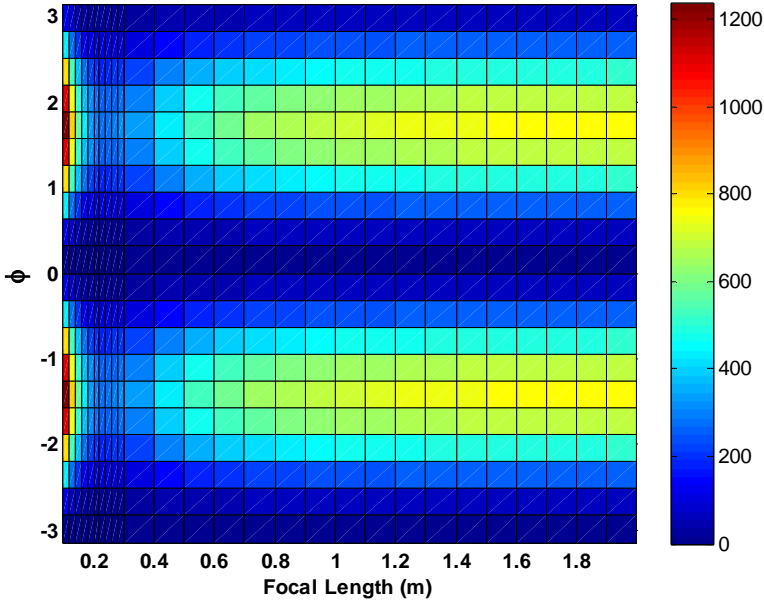
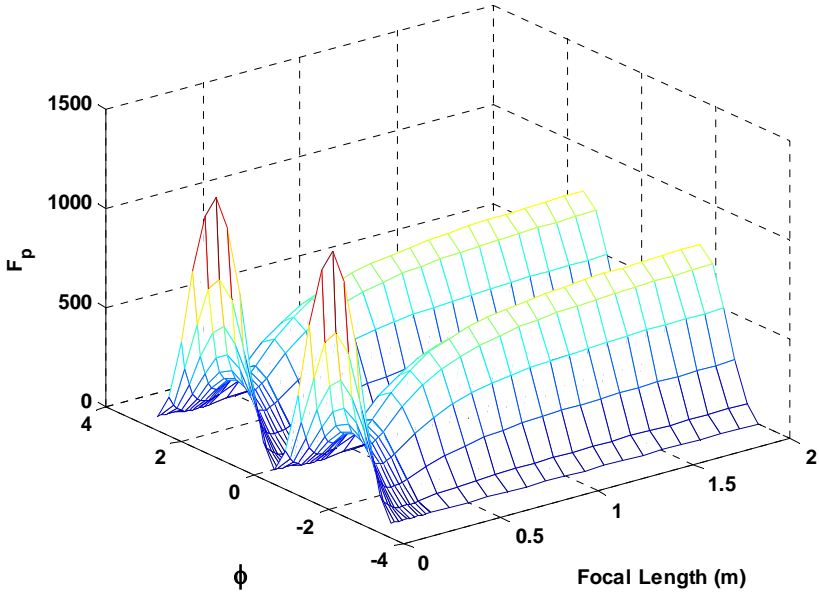


Figure 11b

3.2 The electromagnetic wave source is in the dense medium

The results of calculations are based on the relations (34), (13), (15), (4), (3) and (1). Results of simulations are shown by figures 12a and 12b

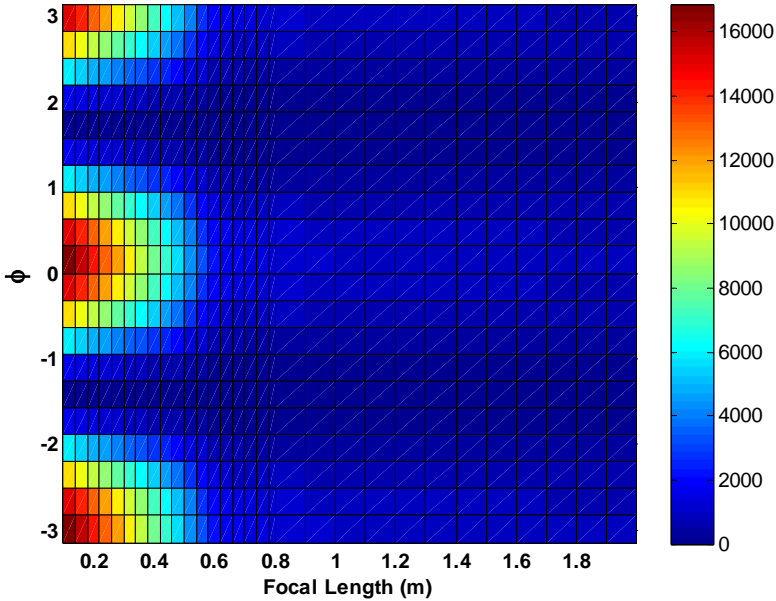
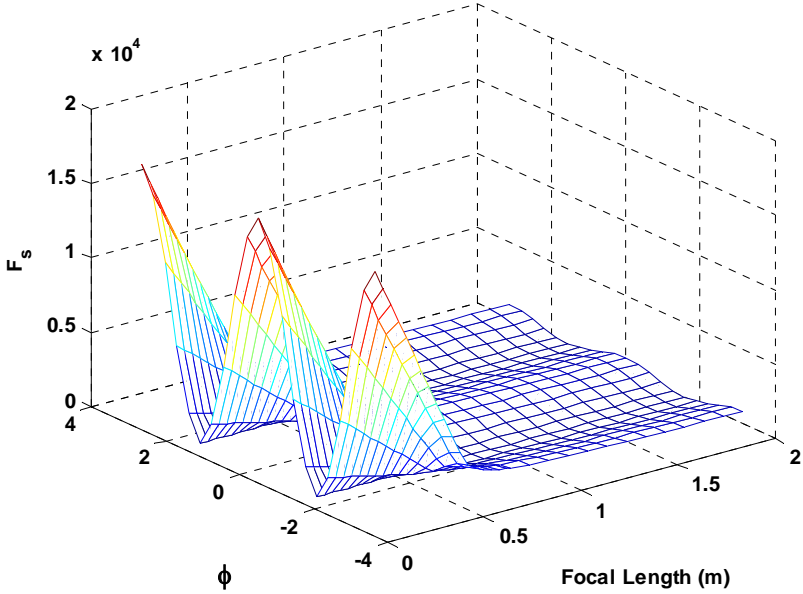


Figure 12a

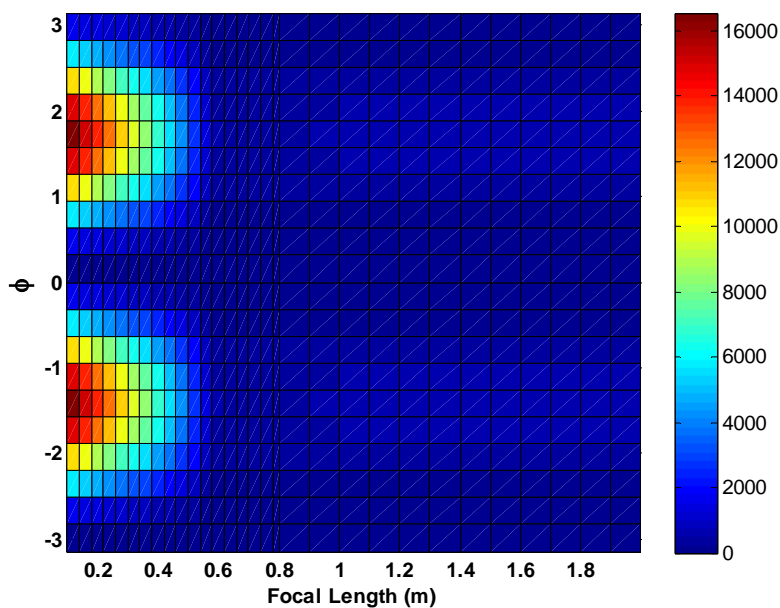
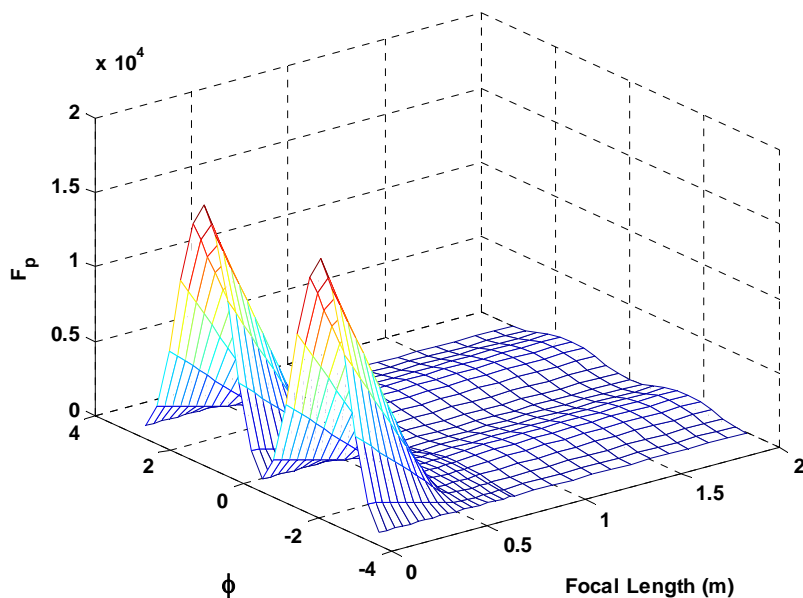


Figure 12b

*3.3 The electromagnetic source of wave is located in the vacuum (parabolic boundary surface is placed between vacuum and conductor)*

Calculations are based on the relations (32) (33) (30), (27), (28), (4), (3) and (1) for S component. For P component calculations are based on the relations (34), (31), (29), (27), (28), (4), (3) and (1). Results of computer programming are shown in figures 13a and 13b.



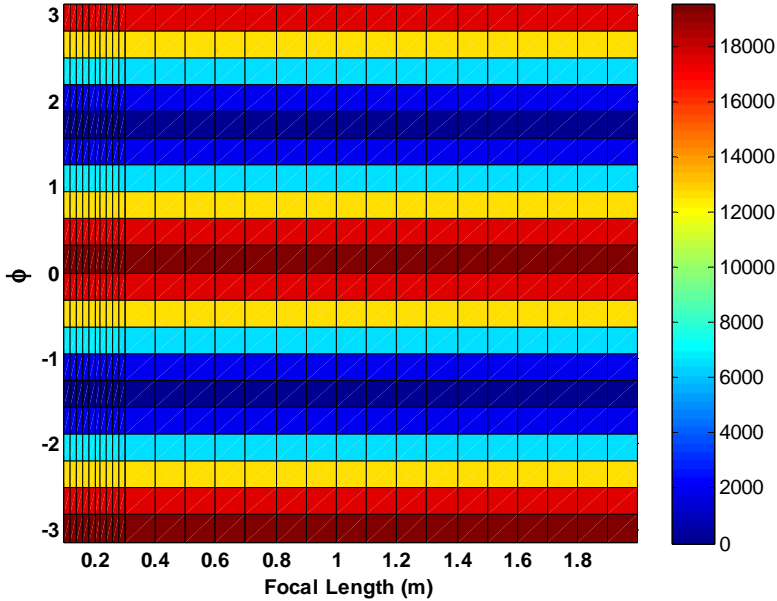
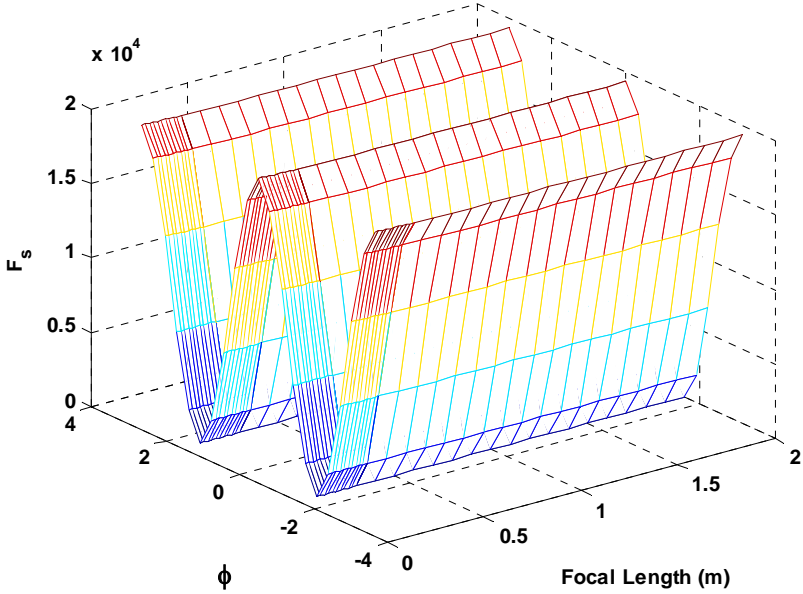


Figure 13a

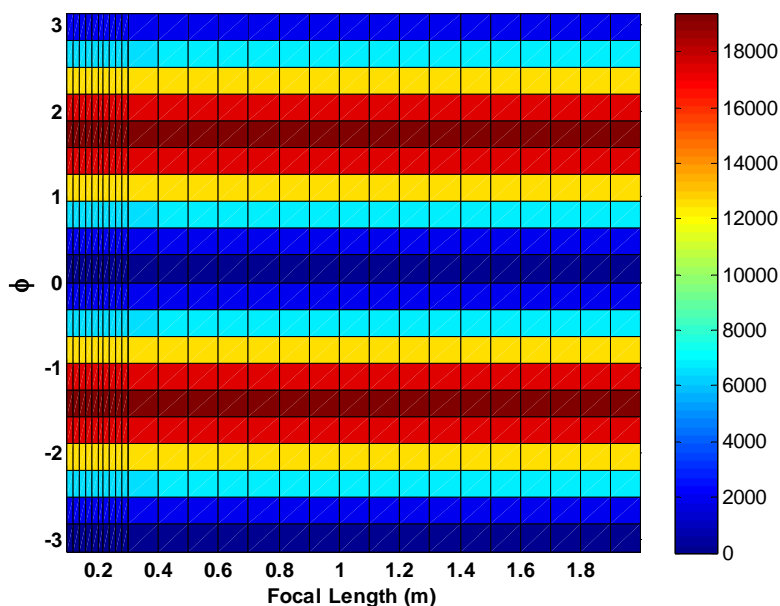
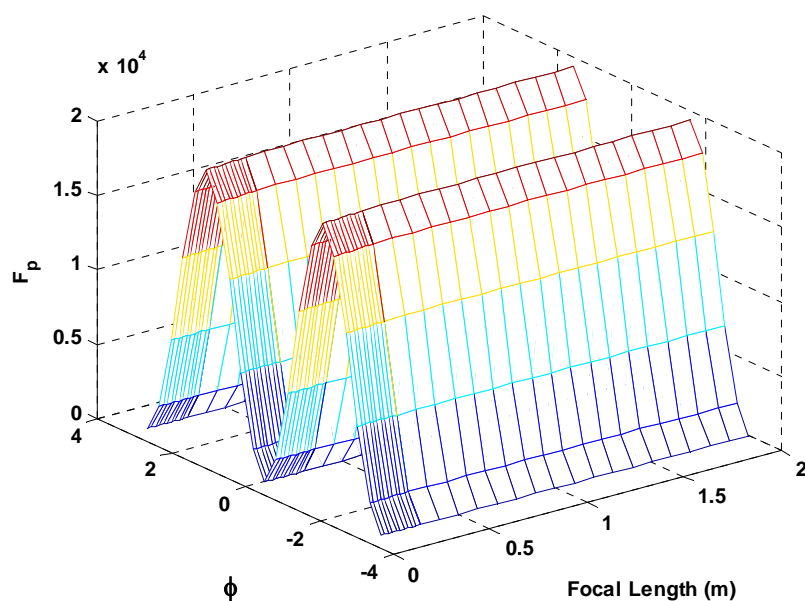


Figure 13b

#### IV. SUMMARY AND CONCLUSION

Parabolic dishes, parabolic mirrors and lenses are used not only in the field of renewable energy but also they are very important tools in the fields of optics, astrophysics, satellite and communications. Curved reflector accessories and lenses are important basic elements for equipments such as radio telescope, reflecting telescope, satellite dishes, solar concentrators, radars and cameras. Without parabolic dishes, parabolic mirrors and lenses we cannot imagine the existence of many high-tech apparatus in human life. In diverse applications of a parabolic reflector, although we consider a definite size for opening of the reflector for a certain incoming power, however the power which is reflected back to the focal point is a function of its focal length and wave polarization (and of course the order of the mediums which are related to incoming and reflected waves). Our investigations show that to the aim of exploiting a parabolic reflector or optical lenses, the power which is reflected back not only depends on the optical features of

the mediums which are separated by curved interface and polarization states of the incoming electromagnetic wave but also it depends on the order of the mediums and the geometrical structure of the curved interface. In the field of solar energy, scientists have tried to optimize the parabolic concentrators and their accessories in different aims from the subject of the current paper (some references are given at the end of this article). However, so far, no one has paid attention to an important key point (optimization on geometrical and electrodynamic features) of such important basic equipments. Results of calculations about optimization of circular parabolic reflectors are published previously by authors [13]. However, optimization of parabolic cylinder interface has been investigated in this article. Simulation has been done in the present paper are showing that if we fix the opening of parabolic cylinder, then due to variation of its focal length the output power would be changed based on the states of polarizations and configuration of parabolic trough with respect to the incoming plane wave. The results of this study are important and would be applicable to the different areas of science and technology such as parabolic and other curved mirrors, satellite receiver antennas, parabolic receivers of radio telescopes, different types of lenses and so on.

#### V. REFERENCES

- [1] Duffie JA, Beckman WA (1991) solar engineering of thermal processes. New York: John Wiley,(chapter1)
- [2] Quaschnig V., Muriel M.B., (2001)“Solar power-Photovoltaic's or Solar thermal power plants, VGB Congress Power plants, Brussels]
- [3] Hatwaambo S., Hakansson H.S, Nilsson and Karlsson B.,2008,“Angular characterization of low Concentrating PV-CPCU sing low- coast Reflectors, Solar energy Materials and solar cells,Vol92 Issue 11,pp.1347-1351]
- [4] Steinfeld A. (2002) solar hydrogen production via two-step water –splitting thermo chemical cycle based on Zn/ZnO redox reaction. International Journal of Hydrogen Energy; 27, 611-619.
- [5] Steinfeld A. (2005) solar thermo chemical production of hydrogen- a review Solar Energy; 78, 603-615.
- [6] Feuermann D, Gordon JM. (1998) solar surgery, remote fiber optic irradiation with highly concentrated sunlight in lieu of lasers, Opt. Eng; 37
- [7] Welford WT, Winston R. (1989) High collection non imaging optics, New York, Academic Press
- [8] Feuermann D, Gordon JM, Ries H. (1999) High-Flux solar concentration with imaging designs, Solar Energy; 65, 83-89
- [9] Steinfeld A, Schubnell M. (1993) Optimum aperture size and operating temperature of a solar cavity-receiver, Solar Energy; 50, 19-25
- [10] Nilson J, Lenutz R, Karlsson B. (2007) Micro-structure reflector surfaces for a stationary asymmetric parabolic solar concentrator. Solar Energy Materials and Solar Cells; 91, 525-533
- [11] Nilson J, Brogren M, Helgesson A, Roos A, Karlsson B. (2006) Biaxial model for the incidence angle dependence of the optical efficiency of photovoltaic systems with asymmetric reflectors. Solar Energy; 80, 1199-1212.
- [12] Brogren M, Helgesson A, Karlsson B, Nilson J, Roos A. (2004) Optical properties, durability and system aspects of a new aluminum-polymer laminated steel reflector for solar concentrator. Solar Energy Materials and Solar Cells, 82, 387-412
- [13] Analysis of reflected intensities of linearly polarized electromagnetic plane waves on parabolic boundary surfaces with different focal lengths, Hossein Arbab, Mehdi Rezagholizadeh (2014) Springer, Journal of Optics.
- [14] Hossein Arbab (2016) A fabrication method for non integrated parabolic mirror based on laser spot image processing and plumbs line, Springer, journal of optics.
- [15] Arbab H, Jazi B, Rezagholizadeh M. (2009) a computer tracking system of solar dish with two-axis degree freedoms based on picture processing of bar shadow. Renewable Energy, 34, 1114-1118.
- [16] Reitz JR, et al. (1979) Foundations of electromagnetic theory. Addison-Wesley publishing company
- [17] Gray DE (1972) American Institute of Physics Handbook New York, McGraw- Hill